Raman Scattering from Surface Phonons in Rectangular Cross-sectional w-ZnS Nanowires

ARTICLE *in* NANO LETTERS · SEPTEMBER 2004

Impact Factor: 13.59 · DOI: 10.1021/nl048720h

NANO LETTERS

2004
Vol. 4, No. 10
1991−1996

Raman Scattering from Surface Phonons in Rectangular Cross-sectional w-ZnS Nanowires

Qihua Xiong,[†,‡] Jinguo Wang,[§] O. Reese,[||] L. C. Lew Yan Voon,[||] and P. C. Eklund*[,†,‡,§]

Department of Physics, Department of Materials Science and Engineering, Material Research Institute, The Pennsylvania State University, University Park, Pennsylvania 16802, and Department of Physics, Wright State University, Dayton, Ohio 45435

Received August 6, 2004; Revised Manuscript Received August 30, 2004

ABSTRACT

Wurtzite (w-) ZnS nanowires with nearly square cross sections have been grown by pulsed laser vaporization of a $(ZnS)_{0.9}Au_{0.1}$ target in a flow of Ar 5%H_2. Growth proceeds by the vapor–liquid–solid mechanism. Raman scattering from the ZnS nanowires in air at room temperature reveals a strong first-order longitudinal optic (LO) phonon (346 cm^{-1}) and two transverse optic (TO) phonons (269 and 282 cm^{-1}), as well as several second-order features. Peak assignments based on bulk ZnS can be made for all the first- and second-order features, except for one band located between the LO and TO bands. This additional Raman band is observed at 335 cm^{-1} in air, and downshifts to 328 cm^{-1} in dichloromethane ($\epsilon_m = 2.0$) and to 326 cm^{-1} in aniline ($\epsilon_m = 2.56$). This band is therefore assigned to surface optic (SO) phonons. The position of the SO band is consistent with a dielectric continuum model for rectangular cross section wires. A symmetry breaking mechanism which may activate the SO mode is also discussed.

In this paper, we report the results of Raman scattering from rectangular cross-section wurtzite ZnS (w-ZnS) nanowires or "nanowaveguides". The Raman spectra show strong first-order phonon peaks and also second-order combination and overtone scattering. The most interesting information in this paper deals with the detection and analysis of Raman-active surface optical (SO) phonons in crystalline nanowires with a rectangular shape, and how the cross-sectional shape of the nanowire affects the position of the SO peak in the spectrum. Furthermore, we argue that a modulation in the nanowire growth rate can produce a modulation in the nanowire cross-sectional area along its length and produce the Raman-active SO phonons. Here we show further evidence[1] that Raman spectroscopy on a polar semiconducting nanowire can provide a simple signature of this growth modulation, and even provides an estimate for the average wavelength of the cross-sectional modulation along the nanowire. Application of a dielectric continuum model for the observed SO modes is discussed, and predictions for both cylindrical and rectangular cross section wires are compared.

Small cross-sectional semiconducting nanowires (SNWs) have been demonstrated as promising "bottom-up" building blocks for nanoscale functional devices and circuits.[2] In principle, they may circumvent the size limits dictated by the "top-down" approach,[3] and research is underway on self-assembly processes that could drive the production of large-scale nanowire devices.[3] A local probe is required to access the quality of the components (i.e., the SNWs). Raman scattering might provide such a probe. The line shape, i.e., peak position and peak width, of the Raman band can yield information concerning the crystalline quality, doping, presence of secondary phase impurities, and crystalline disorder. Furthermore, the Raman scattering of the nanowires themselves, in the limit of small diameter and length, represents a fundamentally important physics problem. One can envision that when the diameter or length of nanowires becomes comparable with the phonon mean free path, phonon confinement will occur and the Raman line shape will change.

Richter[4] proposed a phenomenological model to interpret Raman line shapes in small structures. Fauchet and Campbell[5] extended the model to cylindrical nanowires. According to this model, the selection rule that allows first-order (one-phonon) scattering to take place at the Brillouin zone center (i.e., $q = 0$) is broken, and an asymmetric Raman band with contributions from an extended region of the Brillouin zone occurs.[4,5] Several papers[6] have reported such a change of peak position and line shape. However, Gupta et al.[7] argued

* Corresponding author. E-mail: pce3@psu.edu.
[†] Department of Physics, PSU.
[‡] Department of Materials Science and Engineering, PSU.
[§] Material Research Institute, PSU.
[||] Wright State University.

10.1021/nl048720h CCC: $27.50
Published on Web 09/22/2004

that changes in line shape and peak position in Si nanowires may also be the result of laser heating, and Piscanec et al.[8] also have pointed out that, in order to observe real phonon confinement, inhomogeneous laser heating needs to be ruled out. In this context, phonon confinement normally refers to a "size" effect. On the other hand, a large aspect ratio a, i.e., $a = l/d$, where l is the length and d is the diameter of the nanowires, can lead to a "shape" effect on the phonon spectrum.[9] Mahan et al.[9] have calculated that in high aspect ratio nanowires the long-range dipolar interaction in polar SNWs can give rise to an additional splitting of the LO and TO modes. This occurs because the dipole sums that determine the LO and TO mode frequencies are sensitive to the SNW aspect ratio. Generally, they find that LO_z and TO_z frequencies have the same values as the LO and TO values in the bulk. However, the LO_x and TO_x modes upshift noticeably, where z and x are parallel and perpendicular to the wire axis, respectively. The relative Raman activity of these z and x modes has not been worked out, however, and careful polarization studies need to be carried out to make contact with this theory. Another new result from Raman scattering in SNWs is the observation of surface optic (SO) phonons.[1,10] Detailed investigation and assignment of SO modes were done by Gupta and coauthors[1] in cylindrical cross section GaP nanowires by changing the dielectric constants of the surrounding media in which the wires were embedded. They also identified the symmetry breaking mechanism necessary for activating the SO mode with a diameter modulation along the wire, which arises from an instability in the vapor−liquid−solid (VLS) growth mechanism.[11]

Highly crystalline, rectangular cross-sectional w-ZnS nanowires were grown by laser ablation of a $(ZnS)_{0.9}Au_{0.1}$ target at ~950 °C in a flow of Ar/5%H_2 at a pressure of 225 Torr. As a powder, these nanowires appear to be white, indicating they are a wide band gap material. In another paper based on these same ZnS nanowires,[12] we report band gap luminescence at ~3.70 eV and discuss the effect of wire cross-sectional dimension on the band gap. More detailed information on synthesis, sample preparation, and characterization, e.g., scanning electron microscopy (SEM), X-ray diffraction (XRD), transmission electron microscopy (TEM), and atomic force microscopy (AFM) is also presented in ref 12.

Raman scattering experiments were carried out at room temperature with a JY−Horiba T64000 Raman microscope. The light was focused to a ~1 μm spot and the backscattered light was analyzed using laser excitation at 488 nm. The Raman samples were prepared by putting several drops of a nanowire suspension in 2-propanol onto an indium foil. The 2-propanol was allowed to vaporize at room temperature. The spectra were collected with the sample in air or submerged in various dielectric liquids. The laser power was ~3.0 mW at the sample. The effect of the laser heating was observed to be small at this power, in part, because the SNWs were in good thermal contact with the metallic indium foil.

The as-grown nanowires were confirmed to be wurtzite 2H structure by X-ray diffraction.[12] In Figure 1a, we show

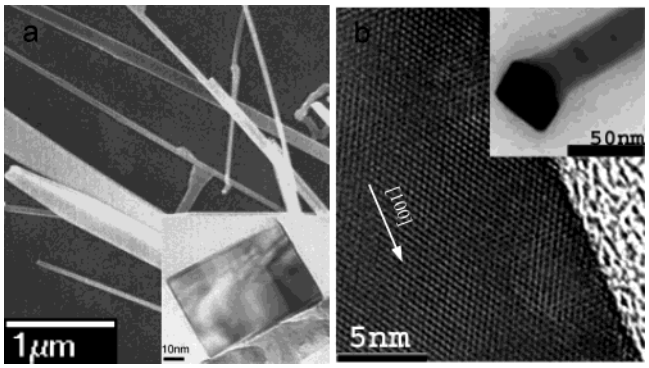

Figure 1. (a) SEM image of ZnS nanowires deposited on Silicon substrate. Inset to the right corner shows a TEM image of the rectangular cross section of our typical ZnS nanowires. (b) High-resolution TEM image of a ZnS nanowire growing along the [100] direction. The inset shows a TEM image of the tip, which is proof of the vapor−liquid−solid mechanism.

an FE-SEM image (JEOL 6700F) of the ZnS nanowires deposited from a 2-propanol solution onto a Si substrate. For the SEM imaging, a thin layer of gold was sputtered over the sample surface to decrease charge accumulation. The inset to Figure 1a shows a TEM image of the rectangular cross section of our typical ZnS wires. Using field-emission SEM (FE-SEM) and TEM, we observed[12] solidified metallic particles on one end of our wires (inset to Figure 1b). This is proof of the VLS growth mechanism. Using energy-dispersive X-ray spectroscopy, the metal particle at the nanowire end was shown to typically be a Au−Zn alloy and very sulfur deficient. Detailed sample preparation and characterization of the cross sections can be found in ref 12. Figure 1b shows a high-resolution TEM (JEOL 2010F) image of an individual ZnS nanowire. From the lattice fringes in this image, and many other images, we can tell the wires are highly crystalline and grow along the ⟨100⟩ and ⟨001⟩ directions (HRTEM images are discussed in more detail in ref 12). Good contrast of the lattice fringes is clearly seen, and the plane spacing is found to be 0.335 nm, which is in good agreement with the lattice spacing between ⟨100⟩ planes found by powder diffraction data of bulk w-ZnS (10-434). The inset to Figure 1b shows a metal particle at the growth end of the nanowire. This particular particle appears faceted, which is not the most prevalent form we observed in many nanowire VLS examples, i.e., most growth "seeds" appear spherical in shape. By TEM and AFM, the nanowires were found to be primarily rectangular and have an average width of ~55 nm (TEM) and average thickness of ~50 nm (AFM).

Wurtzite ZnS has the space group C_{6v}^4 ($C6_3mc$) with two formula units per primitive cell and with all atoms occupying C_{3v} sites. Group theory predicts the following $q = 0$ phonon symmetries: $\chi_{atom} = 1A_1+2B_1+1E_1+2E_2$, while the A_1 and E_1 symmetry phonons are both Raman- and IR-active, the two E_2 pair of modes are only Raman-active, and the two B_1 modes are optically silent.[13] Schneider and Kirby studied the Raman scattering in bulk w-ZnS (2H and 4H) polytypes,[14] while Ebisuzaki and Nicol studied the pressure dependence of Raman scattering in bulk wurtzite 2H ZnS.[15] Brafman and Mitra studied the Raman effect in both wurtzite and zinc

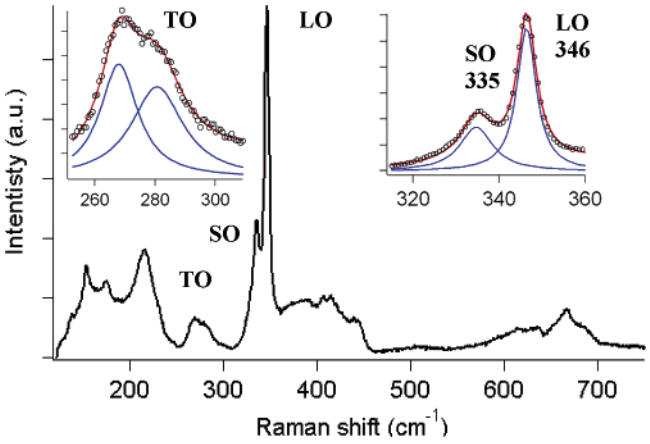

Figure 2. Raman spectrum of ZnS nanowires collected in air ($\epsilon_m = 1$). Two insets show Lorentzian line shape analysis of LO (346 cm^{-1}) and SO (335 cm^{-1}) modes and TO doublet (269, 282 cm^{-1}). Data taken with $\lambda_L = 488$ nm.

Table 1. Assignment of Raman Peaks of ZnS Nanowires in Air at Room Temperature[a]

	frequency (cm^{-1})	
assignment	this work	bulk
LA	216	217[15,16], 219[15]
A_1/E_1(TO)	269	267[14], 273[14,16],274[13], 276[15], 283[14]
E_2(TO)	282	
A_1/E_1(LO)	346.4	348[14], 350[15],351[16],352[13]
SO	335	not observed
2TO	615	617[15]
TO+LA	633	642[15]
2LO	668	673[15]

[a] LA, longitudinal acoustic; TO, transverse optic; LO, longitudinal optic, SO: surface optic.

blende type ZnS single crystals.[16] Also, Arguello and coauthors systematically studied the first-order Raman scattering in several wurtzite crystals including 2H w-ZnS.[13] The bulk data used for comparison in this paper are taken from these four studies.[13−16]

Figure 2 displays a Raman spectrum (100−750 cm^{-1}) of our w-ZnS nanowires. This spectrum was collected in air at room temperature. By analogy to bulk data, strong first-order scattering from an unresolved doublet at 346 cm^{-1} is identified with A_1 and E_1 symmetry LO modes. At lower frequency, a resolvable doublet is seen with peaks at 269 and 282 cm^{-1}. Consistent with the bulk, these peaks are assigned to the A_1 and E_1 TO modes (269 cm^{-1} A_1) and (282 cm^{-1} E_2).[14] An additional feature in the nanowire spectrum, not seen in the bulk spectrum, is observed at 335 cm^{-1}, and this peak is due to surface optic (SO) phonon scattering. We will discuss this assignment later. The two insets to Figure 2 show the results of a Lorentzian line shape analysis for the TO doublet and the nearby LO/SO mode scattering. As also summarized in Table 1, Brafman and Mitra found that E_2 modes are located at 72 and 286 cm^{-1}, whereas the TO modes of A_1 and E_1 symmetry are both located near 273 cm^{-1}. Finally, they assign the LO modes of A_1 and E_1 symmetry to the band at 351 cm^{-1} (ref 16). Arguello and coauthors, on the other hand, found that TO and LO modes were located at 274 cm^{-1} and 352 cm^{-1}, at room temperature,[13] whereas Schneider and Kirby found E_1 (LO) located at 348 cm^{-1}, E_1(TO) at 273 cm^{-1}, and A_1 (TO) at 267 cm^{-1}. Ebisuzaki and Nicol also reported A_1/E_1 LO located at 350 cm^{-1} (ref 15). The broad feature at 216 cm^{-1} in Figure 2 is due to a first-order LA mode according to refs 15 and 16. Our assignments of the LO and TO scattering in our w-ZnS nanowires are consistent with refs 13−16 and they are summarized in Table 1. We also observe continuum scattering in the range 350−450 cm^{-1}, which was also seen by Arguello and coauthors.[13] Peaks in this second-order continuum are usually connected with a 2-phonon density of states (DOS). Schmidt et al.[17] reported second-order Raman scattering in several II−VI semiconductors including w-ZnS. Consistent with their analysis, we can assign our weak broad Raman bands between 600 and 700 cm^{-1} to combination and overtone scattering[15,17] at high 2-phonon DOS (Table 1). The good agreement of our Raman peak positions with the results for bulk w-ZnS confirms that our nanowires exhibit excellent crystal quality and are stoichiometric. Our ZnS nanowires are simply too large in cross section to display phonon confinement effects. Small changes in the LO−TO splitting have been predicted in cubic polar semiconducting nanowires with large aspect ratio.[9] The theory has addressed cubic systems. The general phenomenon of the shape effect is likely to occur in uniaxial polar semiconducting nanowires as well. However, a change in LO−TO splitting in our w-ZnS rectangular cross-sectional wires relative to bulk appears to be small. Without further work, we cannot rule out a small shape effect, however.

The essential characteristic of the Raman-active surface optical (SO) phonon modes is that their peak position and line shape are sensitive to the real part of the dielectric function of the dielectric medium in contact with the surface. Also, if the nanowires have perfect crystal symmetry and a smooth surface, an SO Raman band should not be observed.[1] SO mode scattering must be "activated" by a symmetry breaking mechanism associated with the surface. Indeed, Gupta et al.[1] investigated the change in the SO mode scattering frequency in GaP nanowires as a function of the overlaying media dielectric constant ϵ_m. The nanowire SO band was found between the TO and LO bands and was observed to downshift with increasing ϵ_m. A theoretical model for a cylindrical wire was used to compute the SO mode dispersion $\omega_{SO}(q)$ as a function of ϵ_m. The symmetry breaking mechanism proposed by Gupta et al. is a diameter modulation along the wire due to a VLS growth instability. The dominant wavelength of this modulation was observed in TEM and found to be consistent with the theory for the band position.[1]

Here we present experimental results on the SO modes of *rectangular* cross-sectional ZnS nanowires. The theoretical predictions for the SO modes in rectangular and circular cross section wires differ, as we shall see below. Figure 3a shows the Raman spectra of the SO and LO modes in three different dielectric media air ($\epsilon_m = 1.0$), dichloromethane ($\epsilon_m = 2.0$), and aniline ($\epsilon_m = 2.56$)[1] in which the nanowires were embedded. The band located between the LO and TO bands

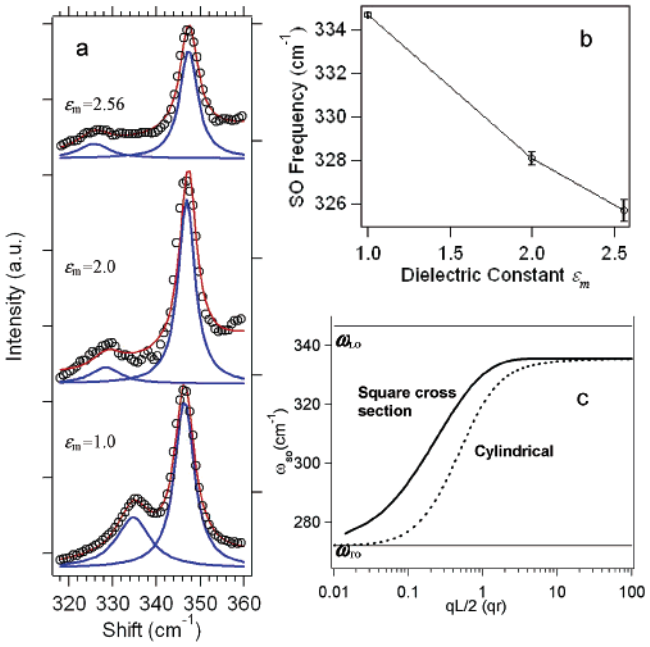

Figure 3. (a) Raman spectra of ZnS nanowires collected in three different media with dielectric constants (ϵ_m). The low- and high-frequency bands are identified with SO and LO phonons. The open circles are the original data and the solid lines are Lorentzian line shape analyses after the least-squares multiple Lorentzian fit. (b) Variation of SO band peak positions as a function of the dielectric constants of the overlaying media. The line is a guide to the eye. (c) Calculated SO dispersions for rectangular wires with square cross sections (solid curve) and a supposed cylindrical ZnS nanowire (dashed curve) with a radius r in air ($\epsilon_m = 1$) using eq 5 and the model in ref 10. Two horizontal lines represent the LO and TO phonon branches, assuming they are dispersionless.

downshifts from 335 cm^{-1} in air, to 328 cm^{-1} in dichloromethane, and to 326 cm^{-1} in aniline, while the LO Raman band remains at the same peak position. Thus, we can unambiguously assign this shifting feature to SO modes. Figure 3b shows the SO band peak position dependence on ϵ_m. The peak position is seen to downshift linearly with increasing ϵ_m. SO modes have also been observed in ZnS nanoparticles by Xu and coauthors using IR spectroscopy.[18] They found that the change of the surface mode peak position is consistent with a macroscopic theory for small spherical crystallites.[19] This model is not suitable to explain our data, since our sample is an ensemble of rectangular cross-sectional nanowires. Although our wires are rectangular, rather than cylindrical in cross section, we nevertheless suspect that they also exhibit the same symmetry breaking mechanism (periodic variation of the cross sectional area) as observed in cylindrical cross-sectional GaP nanowires.[1]

There is no analytical expression for SO modes in rectangular cross section wires. Nevertheless, the dielectric continuum (DC) model approach that was used for cylindrical nanowires[10] remains the most elegant method and, with a small approximation, provides analytical expressions for ω_{SO}(q) vs ϵ_m for rectangular wires. An approximate DC model for rectangular wires was introduced by Stroscio and co-workers[19,20] that neglects the exponentially decaying electrostatic fields eminating from the corner regions. This makes the problem separable in the plane perpendicular to the wire axis and, upon imposition of the usual electrostatic boundary conditions, one obtains the following dispersion relations for the SO phonons:[19]

$$\epsilon_w(\omega)\tanh(q_iL_i/2) + \epsilon_m(\omega) = 0 \tag{1a}$$

$$\epsilon_w(\omega)\coth(q_iL_i/2) + \epsilon_m(\omega) = 0 \tag{1b}$$

Equation 1a is the symmetric mode and eq 1b is the asymmetric mode, $\epsilon_w(\epsilon_m)$ is the dielectric function inside (outside) the wire, $L_i(i = x,y)$ is the edge width of the rectangular wire whose growth direction is along z, and $q_i(i = x,y)$ is the phonon wavevector. We must have[19]

$$q_x^2 + q_y^2 = q^2 \tag{2a}$$

$$q_xL_x = q_yL_y \tag{2b}$$

where eq 2b is the requirement that potentials of optic phonons in the x and y directions should have the same parity.[19] Neglecting the damping and crystal anisotropy, the dielectric function $\epsilon_w(\omega)$ can be expressed as[21]

$$\epsilon_w(\omega) = \epsilon_\infty\frac{\omega_{LO}^2 - \omega^2}{\omega_{TO}^2 - \omega^2} \tag{3}$$

and the Lyddane−Sachs−Teller (LST) relation[21] gives

$$\frac{\epsilon_0}{\epsilon_\infty} = \frac{\omega_{LO}^2}{\omega_{TO}^2} \tag{4}$$

where ϵ_0 and ϵ_∞ are low and high-frequency values of $\epsilon_1(\omega)$, respectively.[22] From eqs 1−4, we can solve for the symmetric (S) and asymmetric (AS) mode SO phonon dispersions:

$$\omega_{SO}^2(q)_S = \omega_{LO}^2\left[\frac{\epsilon_\infty[\epsilon_0\tanh(q_iL_i/2) + \epsilon_m]}{\epsilon_0[\epsilon_\infty\tanh(q_iL_i/2) + \epsilon_m]}\right] = \omega_{TO}^2\left[\frac{\epsilon_0\tanh(q_iL_i/2) + \epsilon_m}{\epsilon_\infty\tanh(q_iL_i/2) + \epsilon_m}\right] \tag{5}$$

$$\omega_{SO}^2(q)_{AS} = \omega_{LO}^2\left[\frac{\epsilon_\infty[\epsilon_0\coth(q_iL_i/2) + \epsilon_m]}{\epsilon_0[\epsilon_\infty\coth(q_iL_i/2) + \epsilon_m]}\right] = \omega_{TO}^2\left[\frac{\epsilon_0\coth(q_iL_i/2) + \epsilon_m}{\epsilon_\infty\coth(q_iL_i/2) + \epsilon_m}\right] \tag{6}$$

w-ZnS is a uniaxial structure, and our wires are growing either along the a axis ([100]) or c axis ([001]) direction. So the crystal anisotropy and the two growth directions would complicate the calculation. Therefore, we use the isotropic eqs 3 and 4. We first evaluate the dispersion relation $\omega_{SO}(q)$ for a square cross-sectional wire in air ($\epsilon_m = 1.0$). For w-ZnS, $\epsilon_{11}(\infty)$ and $\epsilon_{33}(\infty)$ varies from 8.25 to 8.76.[23] As an isotropic approximation, we use $\epsilon_0 = 8.29$, $\epsilon_\infty = 5.11$ from ref 15, and set $\omega_{LO} = 346.5$ cm^{-1}, thus $\omega_{LO} = 272.0$ cm^{-1} using eq

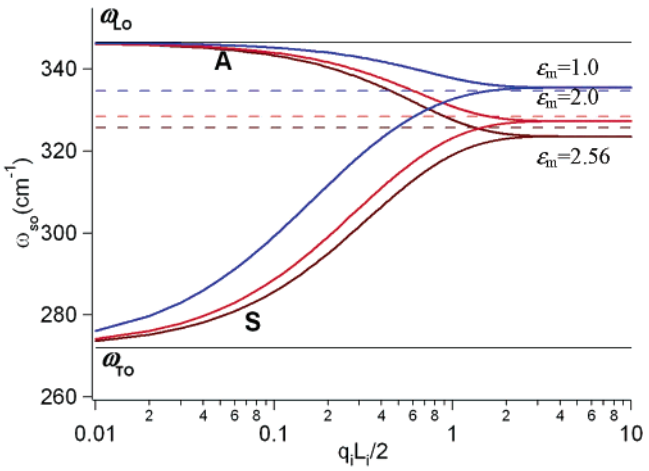

Figure 4. SO phonon dispersion for rectangular cross section wires for three dielectric media calculated from eqs 5 and 6, corresponding to symmetric modes (S) and asymmetric (A), respectively. Three dashed lines represent the measured SO frequencies in air ($\epsilon_m = 1$), dichloromethane ($\epsilon_m = 2$), and aniline ($\epsilon_m = 2.56$). Two horizontal solid lines represent LO and TO frequencies. From the intersection between measured frequency and the corresponding dispersion, we can predict the important wavelength q of the perturbation potential that breaks the symmetry and activates the SO modes.

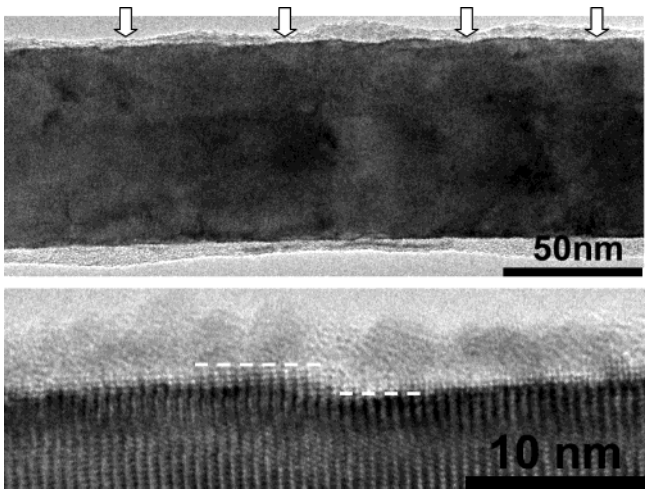

Figure 5. TEM (upper panel) and HRTEM (lower panel) images of ZnS nanowires. Clear surface with a thin amorphous layer was observed. The surface modulation along the wire axis is clearly identified. The hollow arrows indicate the position where the minimum takes place; the average distance between the arrows is about 70 nm. From the HRTEM (lower panel) image, we can estimate that the surface roughness is about several atomic layers (step between dashed lines).

4. In Figure 3c, the solid curve shows an S mode SO phonon dispersion $\omega_{SO}(q)$ vs $qL/2$ for a ZnS nanowires with square cross sections (L_x=L_y=L, thus $q = \sqrt{2}q_i$ $i = x,y$) in air. The experimental SO frequency in air is $\omega_{SO} = 334.7$ cm^{-1}. We can then estimate the important wavevector q of the surface perturbation responsible for activating the SO modes. We find that $qL = 4.55$ is close to the experimental SO frequency (in air). However, if we plot all three **S** mode SO phonon dispersions for three different dielectric media, we find that there are no intersections between experimental SO frequency values and the **S** mode SO phonon dispersions for dichloromethane and aniline (Figure 4). Figure 4 shows a plot of three pair of A/S mode SO phonon dispersion curves in three dielectric media. Each group of A and S modes is represented by the same color. Three dashed horizontal lines represented the SO frequency values (334.7, 328.4, and 325.7 cm^{-1}) observed in the three dielectric media. We find that the intersections are on the A mode SO dispersion curves, which yield $qL = 4.53$ in dichloromethane and $qL = 3.82$ in aniline. We can see that the q values obtained from air and dichloromethane are self-consistent, while there is little discrepancy in aniline. However, if we take the same qL value (~4.55), the A mode SO dispersion in aniline predicts an SO phonon frequency ~324.8 cm^{-1}, only 0.9 cm^{-1} lower than the experimental value. We believe this 0.9 cm^{-1} difference is consistent with the error in our SO frequency measurement, i.e., $\Delta w_{SO} = \pm$ 0.5 cm^{-1}. If we take the average wire square cross section dimensions to be 50 × 50 nm^2, we can then calculate the wavelength for the surface potential perturbation that breaks the symmetry and activates the SO mode Raman scattering, i.e., $\lambda = 2\pi/q \approx 70$ nm.

It is also interesting to compute the SO mode dispersion for a cylindrical ZnS nanowire (diameter d) and compare the results to what we observe for our rectangular wires when $d = L$. In Figure 3c, the dashed curve shows the calculated SO dispersion for cylindrical ZnS nanowires in air. We have used the model described in ref 1. From the measured SO frequency in air, e.g., $\omega_{SO} = 334.7$ cm^{-1} and using the SO dispersion in Figure 3c, we can estimate the important wavevector q responsible for activating the SO modes. We find that $qd = 25$ predicts the experimental SO frequency in air. The wavelength for the perturbation is therefore $\lambda = 2\pi/q \approx 13$ nm. This λ differs by a factor of about 5 from the λ obtained from the rectangular cross section SO analysis. So it is clear that the correct nanowire shape must be used in the analysis. The importance of the effect of the nanowire shape on the SO analysis is clear from Figure 3c.

The TEM and HRTEM images (Figure 5) indeed show that the surface modulation prevails along the wire axis. The surface modulation, however, in this case appeared to be not as clearly periodic as in cylindrical nanowires.[1] Nevertheless, we can still confirm that the theoretical calculations based on the dielectric continuum model are consistent with our TEM images; i.e., we believe the important wavelength of the perturbation that breaks the symmetry and activates SO mode is ~70 nm. Furthermore, from the HRTEM image (lower panel) we can estimate that the surface roughness is approximately several atomic layers.

The LO and TO Raman band line width is known to be very sensitive to the crystalline order of the material. The full width at half-maximum (fwhm) of the first-order LO band of our wires at 300 K is ~4 cm^{-1} corrected for the instrument resolution. This is a reasonable linewidth at 300 K. We have not found any other data on the natural width of the LO band in bulk crystalline material. We should also mention that we have compared our Raman spectrum with that of cubic ZnS[24] and other possible wurtzite polytypes (e.g., 4H),[14] and we do not observe any of the characteristic strong Raman bands identified with either c-ZnS[24] or 4H

w-ZnS.[14] This is further testimony to the quality of our PLV grown nanowires and is consistent with our X-ray diffraction data.[12]

In summary, highly crystalline ZnS rectangular cross-sectional wires have been synthesized by pulsed laser vaporization. These nanowires typically have a square cross section $\sim 50 \times 50\ \mu m^2$ and a length of $\sim 10\ \mu m$. Systematic study of the Raman scattering from these nanowaveguide wires at room temperature in air have resolved strong first-order LO, TO, and SO modes and second-order combinations and overtones. The SO band is identified by its movement in surrounding dielectric media. Using an analytical dielectric continuum (DC) model for rectangular cross section wires, we predict that a strong modulation of the nanowire diameter with a $\lambda \sim 70$ nm would provide the symmetry breaking mechanism necessary to observe the SO band at 335 cm^{-1} in air.

Acknowledgment. This work was supported by NFS-NIRT (Nanotechnology and Interdisciplinary Research Initiative), grant DMR-0304178. We thank Prof. Elizabeth Dickey for discussion on TEM. L.Y.V. was supported by NSF-CAREER, grant DMR-9984059.

References

(1) Gupta, R.; Xiong, Q.; Mahan, G. D.; Eklund, P. C. *Nano Lett.* **2003**, *3*(12), 1745.
(2) Cui, Y.; Lieber, C. M. *Science* **2001**, *291*(5505), 851. Duan, X. F.; Huang, Y.; Cui, Y.; Wang, J. F.; Lieber, C. M. *Nature* **2001**, *409*(6816), 66. Huang, Y.; Duan, X. F.; Cui, Y.; Lauhon, L. J.; Kim, K. H.; Lieber, C. M. *Science* **2001**, *294*(5545), 1313.
(3) Samuelson, L. *Materials Today* **2003**, *6*(10), 22.
(4) Richter, H. *Solid State Commun.* **1981**, *39*, 625.
(5) Campbell, I. H.; Fauchet, P. M. *Solid State Commun.* **1986**, *58*(10), 739.
(6) Li, B. B.; Yu, D. P.; Zhang, S. L. *Phys. Rev. B* **1999**, *59*(3), 1645. Wang, R. P.; Zhou, G. W.; Liu, Y. L.; Pan, S. H.; Zhang, H. Z.; Yu, D. P.; Zhang, Z. *Phys. Rev. B* **2000**, *61*(24), 16827.
(7) Gupta, R.; Xiong, Q.; Adu, C. K.; Kim, U. J.; Eklund, P. C. *Nano Lett.* **2003**, *3*(5), 627.
(8) Piscanec, S.; Cantoro, M.; Ferrari, A. C.; Zapien, J. A.; Lifshitz, Y.; Lee, S. T.; Hofmann, S.; Robertson, J. *Phys. Rev. B* **2003**, *68*(24), 241312(R).
(9) Mahan, G. D.; Gupta, R.; Xiong, Q.; Adu, C. K.; Eklund, P. C. *Phys. Rev. B* **2003**, *68*(7), 073402.
(10) Lin, H. M.; Chen, Y. L.; Yang, J.; Liu, Y. C.; Yin, K. M.; Kai, J. J.; Chen, F. R.; Chen, L. C.; Chen, Y. F.; Chen, C. C. *Nano Lett.* **2003**, *3*(4), 537.
(11) Givargizov, E. I. *J. Cryst. Growth* **1973**, *20*, 217.
(12) Xiong, Q.; Chen, G.; Accord, J. D.; Liu, X.; Gutierrez, H.; Redwing, J. M.; Lew Yan Voon, L. C.; Lassen, B.; Eklund, P. C. *Nano Lett.* **2004**, *4*(9), 1663.
(13) Arguello, C. A.; Rousseau, D. L.; Porto, S. P. S. *Phys. Rev.* **1969**, *181*(3), 1351.
(14) Schneider, J.; Kirby, R. D. *Phys.Rev. B* **1972**, *6*(4), 1290.
(15) Ebisuzaki, Y.; Nicol, M. *J. Phys. Chem. Solids* **1971**, *33*, 763.
(16) Brafman, O.; Mitra, S. S. *Phys. Rev.* **1968**, *171*(3), 931.
(17) Schmidt, R. L.; Kunc, K.; Cardona, M.; Bilz, H. *Physical Review B* **1979**, *20*(8), 3345.
(18) Xu, J. F.; Mao, H. T.; Sun, Y.; Du, Y. W. *J. Vac. Sci. Technol. B* **1997**, *15*(4), 1465.
(19) Stroscio, M. A.; Kim, K. W.; Littlejohn, M. A.; Chuang, H. H., *Phys. Rev. B* **1990**, *42*(2), 1488.
(20) Stroscio, M. A.; Dutta, M.; ebrary Inc., *Phonons in nanostructures*.; Cambridge University Press: Cambridge; New York, 2001.
(21) Yu, P. Y.; Cardona, M. *Fundamentals of semiconductors: physics and materials properties*, 2nd updated ed. (Springer, Berlin; New York, 1999)
(22) ϵ_∞ and ϵ_0 refer, respectively, to the value of $\epsilon(\omega)$ for ω just below $E_g/\hbar$ and near zero frequency. They also represent an isotropic average over all crystal directions.
(23) Dan'kov, I. A.; Kobyakov, I. B.; Davydov, S. Y. *Sov. Phys. Solid State* **1982**, *24*(12), 2058.
(24) Nilsen, W. G. *Physical Review* **1969**, *182*(3), 838.

NL048720H